DOI: 10.1002/ejoc.201301243

Development of a Benzimidazole-Derived Bidentate P,N-Ligand for Enantioselective Iridium-Catalyzed Hydrogenations

Jarno J. M. Weemers,[a] Fanni D. Sypaseuth,[a] Patrick S. Bäuerlein,[a] William N. P. van der Graaff,[a] Ivo A. W. Filot,[a] Martin Lutz,[b] and Christian Müller*[a,c]

Keywords: Ligand design / N,P ligands / Asymmetric catalysis / Hydrogenation / Iridium / Nitrogen heterocycles / Kinetic resolution

The development of a novel benzimidazole-derived bidentate P,N-ligand and its application in Ir-catalyzed hydrogenation is described. The ligand backbone was obtained through a one-pot tandem hydroformylation–cyclization sequence and the enantiomers of the generated alcohol were separated by chiral HPLC. By comparing the experimentally obtained CD spectra of the enantiomers with the simulated spectra generated from time-dependent DFT calculations, the absolute configuration could be obtained. The chiral alcohols could further be isolated on a larger scale after transesterification by using *Candida Antarctica* lipase B (Novozym 435) and could subsequently be converted into the corresponding chiral P,N-ligand by reaction with $ClPPh_2$. The coordination properties of the racemic P,N-ligand were investigated and the molecular structure of the Rh^I complex [(P,N)Rh(CO)Cl] was determined by X-ray crystal structure analysis. The corresponding chiral cationic Ir^I complex was used as catalyst for the enantioselective hydrogenation of prochiral *N*-phenyl-(1-phenylethylidene)amine and *trans*-α-methylstilbene. For the *N*-aryl-substituted imine, enantiomeric excesses of only 10 % were obtained, whereas the unfunctionalized olefin could be hydrogenated with enantiomeric excesses of up to 90 %. Interestingly, the modular synthetic access to the P,N-hybrid system described here allows facile modification of the ligand structure, which should extend the scope of such novel P,N-ligands for asymmetric catalytic conversions to a large extent in the future.

Introduction

The enantioselective hydrogenation of prochiral substrates is one of the most important and efficient asymmetric catalytic transformations for the pharmaceutical industry, the production of fine chemicals, as well as for academia.[1] Enantioselective hydrogenations of chelating prochiral alkenes based on cationic rhodium systems have been well-studied.[2] On the other hand, the hydrogenation of C=N double bonds and nonfunctionalized prochiral alkenes, which lack polarized double bonds and bear functional groups that do not coordinate to the metal center, is currently of special interest but still remains a challenge.[3] For this reaction, iridium complexes based on chiral P,N-ligands are particularly well-suited, however, access to such ligand systems is often not trivial.

Crabtree was the first to describe the remarkable catalytic activities of (pyridine)(phosphine)iridium complexes in the hydrogenation of variously substituted olefins (Figure 1, **A**).[4] Later, the application of chiral bidentate P,N-ligands in iridium-catalyzed hydrogenation was pioneered by Pfaltz and co-workers[5] (**B** and **C**). Since then, major contributions in the areas of ligand design as well as the application of more challenging substrate classes have been made by the groups of Burgess,[6] Andersson (**D**),[7] and others.[8]

P,N-Hybrid ligands (Figure 1) consist of a phosphorus atom, which acts as a "soft" donor towards a metal center and is able to stabilize metals in lower oxidation states. The nitrogen atom, on the other hand, stabilizes metals in higher oxidation states due to its "hard" donor characteristics. Such mixed donor ligands show a potentially hemilabile behavior that depends on the oxidation state of the metal center in the catalytic cycle, and one donor atom can be more strongly bound than the other. Although monodentate phosphines were the first chiral ligands to be prepared and applied in the enantioselective catalytic hydrogenation, the use of bidentate ligands resulted in far superior enantioselectivities. Research on monodentate ligands, however, has increased over the last ten years. De Vries and co-workers[9] demonstrated excellent enantioselectivities of acyclic *N*-aryl imines with an iridium catalyst based on the monodentate phosphoramidite PipPhos (Figure 1, **E**). The

[a] Chemical Engineering and Chemistry, Eindhoven University of Technology,
Den Dolech 2, 5600 MB Eindhoven, The Netherlands
[b] Bijvoet Center for Biomolecular Research, Crystal and Structural Chemistry, Utrecht University,
Padualaan 8, 3584 CH Utrecht, the Netherlands
[c] Institut für Chemie und Biochemie – Anorganische Chemie, Freie Universität Berlin,
Fabeckstr. 34/36, 14195 Berlin, Germany
E-mail: c.mueller@fu-berlin.de
http://www.bcp-fu-berlin.de/ak-mueller
Supporting information for this article is available on the WWW under http://dx.doi.org/10.1002/ejoc.201301243.

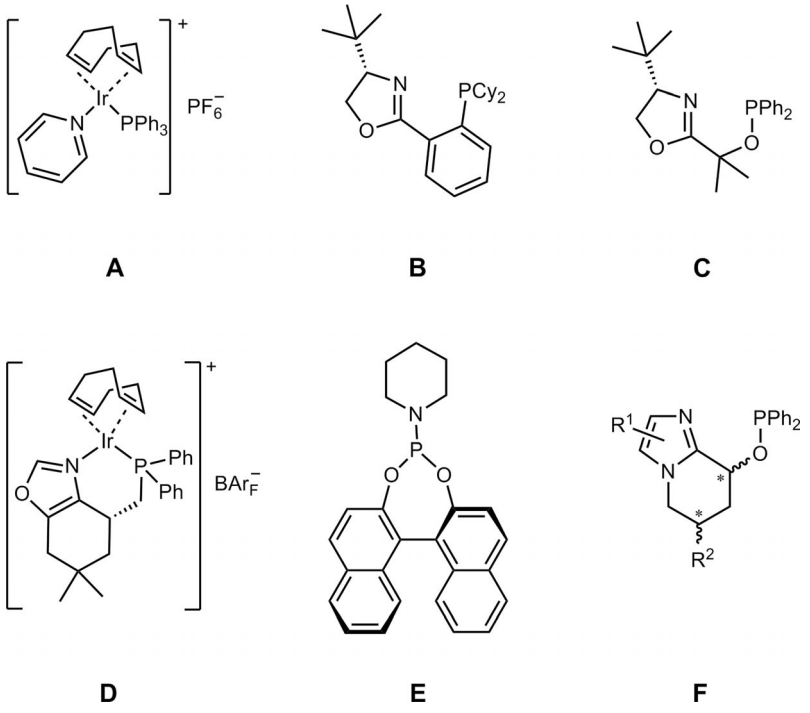

Figure 1. Selected examples of ligands and complexes for iridium-catalyzed hydrogenation.

focus on new ligand classes was further extended by Burgess and co-workers, who successfully applied NHC carbene-based C,N/Ir^+ catalysts in the asymmetric hydrogenation of aryl alkenes.[6c–6e]

Recently, we reported on the selective formation of hydroxy-functionalized bicyclic imidazole **G** through a tandem type hydroformylation–cyclization sequence starting from a methylallyl heteroaromatic substrate (Scheme 1).[10]

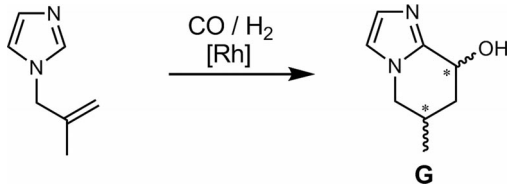

Scheme 1. Tandem type one-pot hydroformylation–cyclization sequence for the formation of chiral bicyclic methyl-substituted benzimidazole-based alcohol **G**.

Interestingly, the core structure of the generated heterocycles is found in biologically active compounds such as nagstatins. Moreover, we realized that they can also serve as chiral building blocks for the preparation of a new class of imidazole-based P,N-ligands (Figure 1, **F**) and are therefore potentially relevant for both pharmaceutical and fine chemistry applications. As a matter of fact, this new type of system has a striking resemblance to previously reported (chiral) ligands;[4–8] they all contain both a phosphorus and a nitrogen donor atom and form six-membered chelate-rings upon coordination to an iridium metal center.

Here, we report on the design, synthesis, and characterization of a novel type of tricyclic benzimidazole-based P,N-ligand and present a first example of its application in the asymmetric iridium-catalyzed hydrogenation of an *N*-aryl imine and an unfunctionalized olefin substrate.

Results and Discussion

Stimulated by our recent results, we started to investigate the scope of the hydroformylation–cyclization sequence and synthesized the methylallyl-functionalized benzimidazole derivative **1** (Scheme 2). This compound was prepared in a one-step reaction starting from benzimidazole and commercially available 3-chloro-2-methylpropene and was obtained in good yield after workup. Substrate **1** was subsequently hydroformylated in toluene as solvent at 120 °C in CO/H_2 (1:1, 20 bar) in the presence of a catalytic system based on [Rh(acac)$(CO)_2$] and a phosphabarrelene (Scheme 2).[10]

After 45 h, **1** was almost completely converted and product **3** was collected as a white solid after recrystallization from hot tetrahydrofuran (THF) or toluene. Figure 2 shows the distribution-of-species plot generated during the hydroformylation–cyclization sequence.

The crystalline material was analyzed by means of chiral HPLC and it was possible to separate the four stereoisomers, resulting from the implementation of two stereogenic centers during the formation of **3** from **1**. From the integrals of the signals, a diastereomeric ratio of 1:3 could be concluded (Figure 3).

Analysis of **3** by ^1H NMR spectroscopy revealed the characteristic resonance of the proton adjacent to the OH-functionality at δ = 5.0–5.3 ppm as well as the resonance of the proton of the OH group at δ = 5.9–6.3 ppm. The same ratio of diastereomers in the diastereomeric mixture was observed as determined by HPLC analysis (Figure 4).

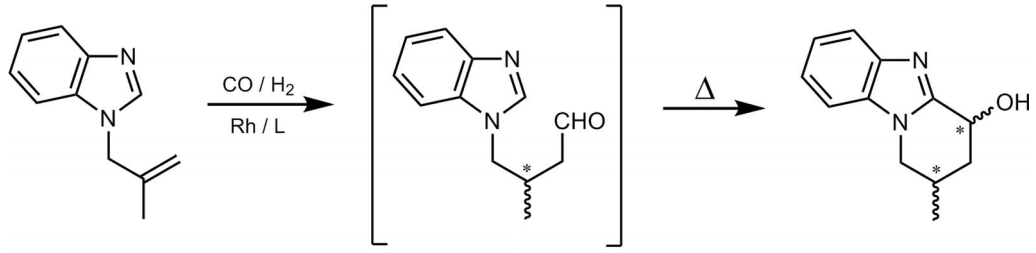

Scheme 2. Tandem hydroformylation–cyclization sequence for the formation of benzimidazole-based alcohol **3**.

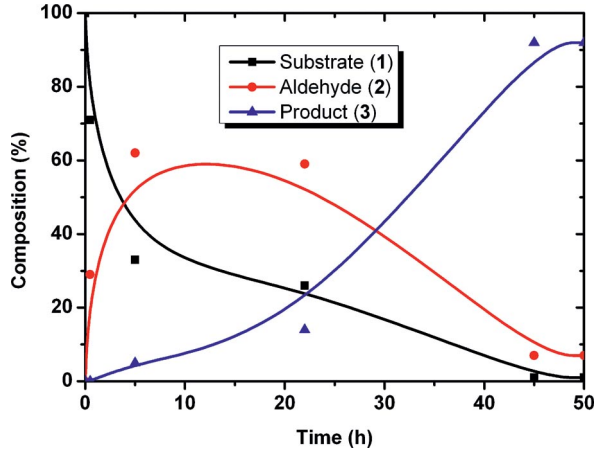

Figure 2. Distribution of species plot for the one-pot tandem hydroformylation-cyclization reaction of **1**. Reaction conditions: 120 °C, 20 bar (CO/H_2 = 1:1), THF, V_{tot} = 8.0 mL, Rh/L/S = 1:20:1500, substrate (12.0 mmol, 1.5 mL), $[Rh(acac)(CO)_2]$, phosphabarrelene.[10]

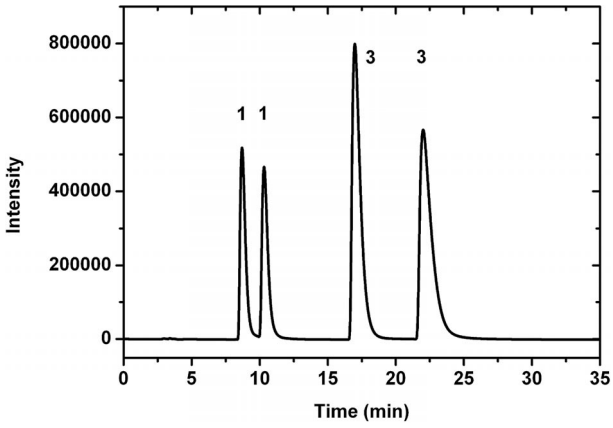

Figure 3. HPLC analysis of baseline separation of both diastereomeric pairs of **3** (ratio 1:1:3:3) by using analytical HPLC on a chiral stationary phase with *n*-hexane/2-propanol (98:2) as the eluent (Chiralcel OJ-H; t_1 = 8.70, t_2 = 10.32, t_3 = 16.98, t_4 = 22.01 min; T = 25 °C; flow rate: 1.0 mL/min; λ = 254 nm).

Racemic single crystals of **3** that were suitable for X-ray diffraction were obtained by crystallization from hot THF; the molecular structure of the *syn*-stereoisomer in the crystal is depicted in Figure 5 (a). By hydrogen bonding with

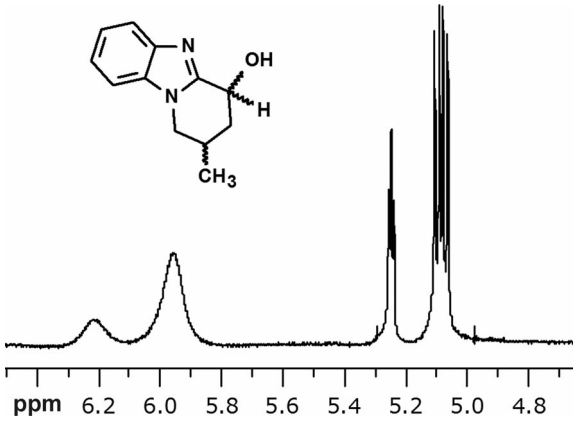

Figure 4. ^1H NMR (400.16 MHz, $CDCl_3$, 25 °C) spectrum of the diastereomeric mixture of **3**.

the OH group as donor and N(1) as acceptor, centrosymmetric dimers were formed in the crystal (Figure 5, b). From Figure 3 it is clear that a separation of all four stereoisomers into diastereomerically pure compounds by (semi)-preparative HPLC would be difficult to achieve, even under optimized conditions. We therefore decided to simplify the target molecule by excluding the methyl group connected to C(2) (Scheme 3), and thus reduce the number of possible stereoisomers.

As a starting point for the one-pot tandem type hydroformylation–cyclization sequence, allyl-substituted benzimidazole **4** was chosen as substrate, which could be synthesized in one step by reaction of benzimidazole with allyl bromide. Because **4** lacks a methyl group on the β-position of the double bond, in contrast to compound **1**, the number of stereoisomers is reduced from two enantiomeric pairs to only one enantiomeric pair. Compound **4** was hydroformylated in the first step to the intermediate aldehyde **5** at 120 °C with syngas (20 bar, CO/H_2 = 1:1) by using $[Rh(acac)(CO)_2]$ as metal precursor and Xantphos as ligand (Scheme 3).

This chelating diphosphine is known to direct the hydroformylation reactions towards the desired linear product.[11] We anticipated that the subsequent ring-closing reaction would finally generate racemic alcohol **6**, according to Scheme 3. From the distribution-of-species plot shown in Figure 6 it became clear, however, that the hydroformylation–cyclization sequence in the case of substrate **4** was

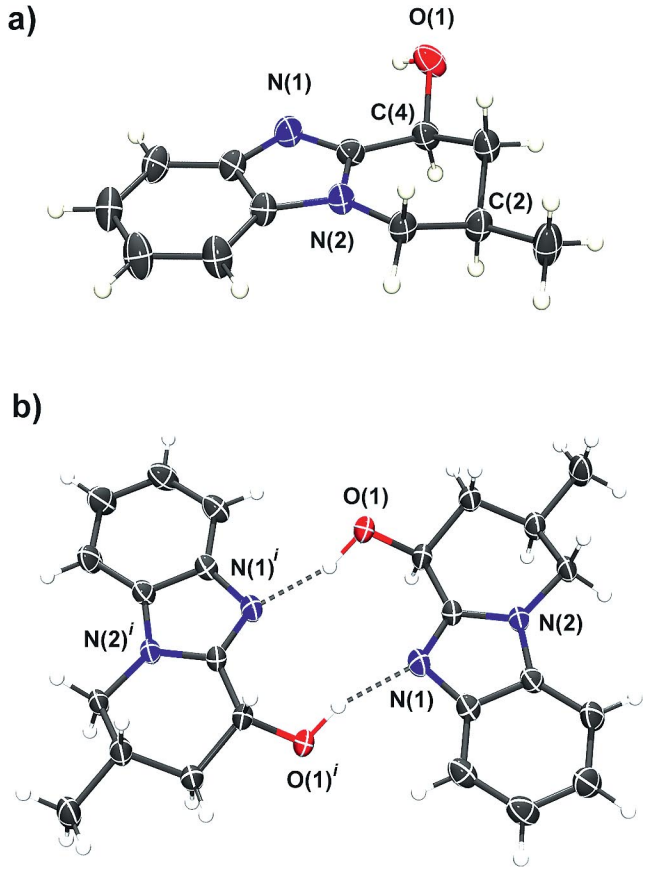

Figure 5. Molecular structure of **3** in the crystal. Displacement ellipsoids are shown at the 50% probability level. (a) Stereoisomer (*R*,*S*)-**3** (b) Hydrogen bonding between two adjacent molecules. Symmetry operation *i*: 1 – *x*, 1 – *y*, 1 – *z*.

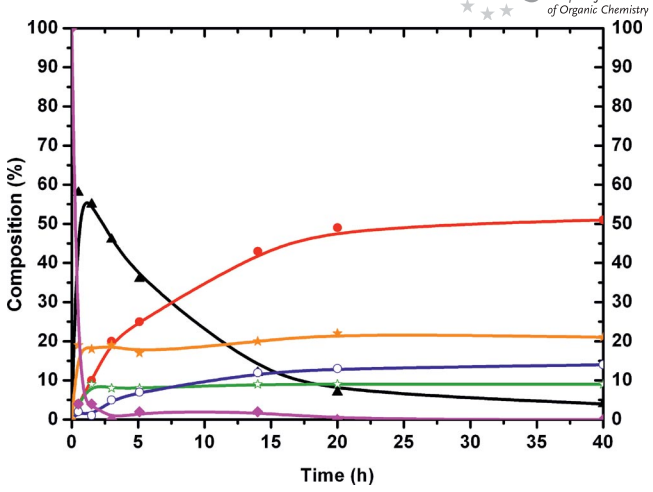

Figure 6. Distribution-of-species plot for the one-pot tandem hydroformylation–cyclization reaction of **4**. Reaction conditions: 120 °C, 20 bar (CO/H_2 = 1:1), toluene, V_{tot} = 8.0 mL, Rh/L/S = 1:4:1500, substrate (12.0 mmol, 2.07 g), $[Rh(acac)(CO)_2]$, Xantphos.

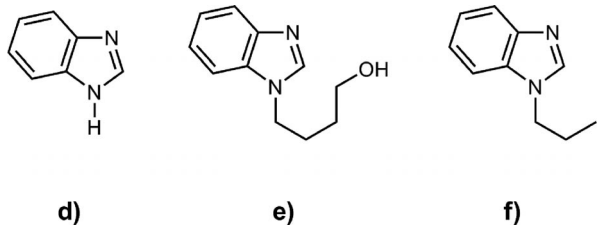

Figure 7. Additional byproducts formed during the one-pot tandem hydroformylation–cyclization reaction of **4**.

less selective than for **1**. In addition to the formation of the desired benzimidazole-based secondary alcohol **6**, three additional byproducts **d**–**f** were observed.

Analysis of the product mixture by GC–MS revealed that not only had the hydrogenated product, *N*-propylbenzimidazole (**f**), formed but also the alcohol corresponding to the linear aldehyde (**e**), and even benzimidazole (**d**) was detected in relatively large amounts (ca. 21%) (Figure 7).

From Figure 6 it is clear that consumption of substrate **4** is very fast, because almost full conversion was accomplished within 30 minutes. At that time, the maximum concentration of aldehyde **5** was reached, accounting for 58% of the total composition. In the same period of time, about 20% of the substrate was converted into benzimidazole **d**, and another 9% was hydrogenated to give **f**. The aldehyde was slowly converted into the ring-closed product. This reaction, however, is in competition with the hydrogenation of the aldehyde to the alcohol **e**. After 40 hours, the aldehyde is almost fully converted, and the ring-closed product **6** and alcohol **f** make up 51 and 14% of the reaction mixture, respectively. The formation of benzimidazole is remarkable; the reductive cleavage of the N–C bond is probably due to a deprotection reaction in which the allyl group is cleaved, forming benzimidazole and propene. As a matter of fact, compound **d** seems not to be generated from aldehyde **5**, but is instead formed rapidly at the very beginning of the substrate conversion, with its concentration subsequently remaining constant during the course of the reac-

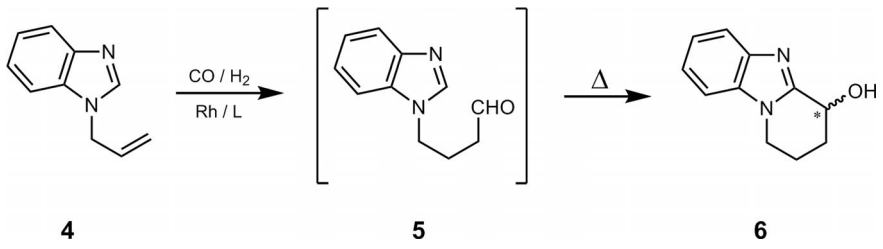

Scheme 3. Tandem hydroformylation–cyclization sequence for the formation of tricyclic benzimidazole-based alcohol **6**. L = Xantphos, Rh = $[Rh(acac)(CO)_2]$.

tion. The deallylation process of allylamines is known to be catalyzed by transition-metal complexes (most notably rhodium and ruthenium).[12,13]

After cyclization of the linear aldehyde, a racemic mixture of chiral tricyclic alcohol **6** was formed. Even though a product mixture was generated during the hydroformylation–cyclization sequence, **6** could easily be isolated as a highly pure, white solid or as colorless crystals after combined flash column chromatography and recrystallization of the mixture from hot THF or toluene. The racemic alcohol was analyzed by ^{1}H and $^{13}C\{^{1}H\}$ NMR spectroscopy as well as by chiral HPLC. The ^{1}H NMR spectrum of **6** along with the HPLC chromatogram is depicted in Figure 8.

We then considered whether it was possible to transform compound **6** into a novel P,N-hybrid ligand, and found that racemic tricyclic alcohol **6** could indeed be easily converted into the corresponding racemic P,N-ligand **7** by reaction with chlorodiphenylphosphine in the presence of NEt_3. Compound **7** was isolated as a white solid in 76% yield after filtration (Scheme 4).

To verify the structure of this novel type of hemilabile P,N-ligand, we investigated the coordination behavior of *rac*-**7** towards $[Ir(COD)_2]BF_4$ and $[Ir(COD)_2]BAr_F$ (Scheme 5). Both reactions resulted in a single resonance in the $^{31}P\{^{1}H\}$ NMR spectra (δ = 102.7 ppm and δ = 105.4 ppm, respectively). Unfortunately, all attempts to obtain crystals from the above mentioned complexes failed. Nonetheless, reaction of *rac*-**7** with the Rh-dimer $[Rh(CO)_2Cl]_2$ was successful, and yellow crystals that were suitable for X-ray diffraction could be obtained from [(*rac*-**7**) Rh(CO)Cl] by slow diffusion of Et_2O into a CH_2Cl_2 solution of the complex (Figure 9).

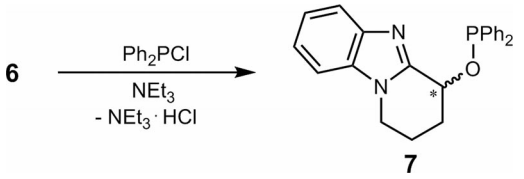

Scheme 4. Synthesis of racemic P,N-ligand **7** from racemic tricyclic alcohol **6**.

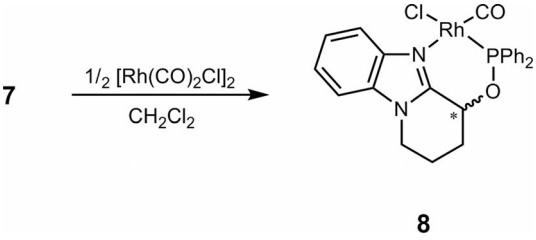

Scheme 5. Synthesis of complex **8**.

Rh complex **8** crystallized as a racemate in the triclinic space group $P\bar{1}$ (no. 2) and the molecular structure along with selected bond lengths and angles is shown in Figure 9. The rhodium atom displays a square-planar geometry, which is typical for a 16-electron complex. The planarity of the benzimidazole part is clearly visible as well as the non-

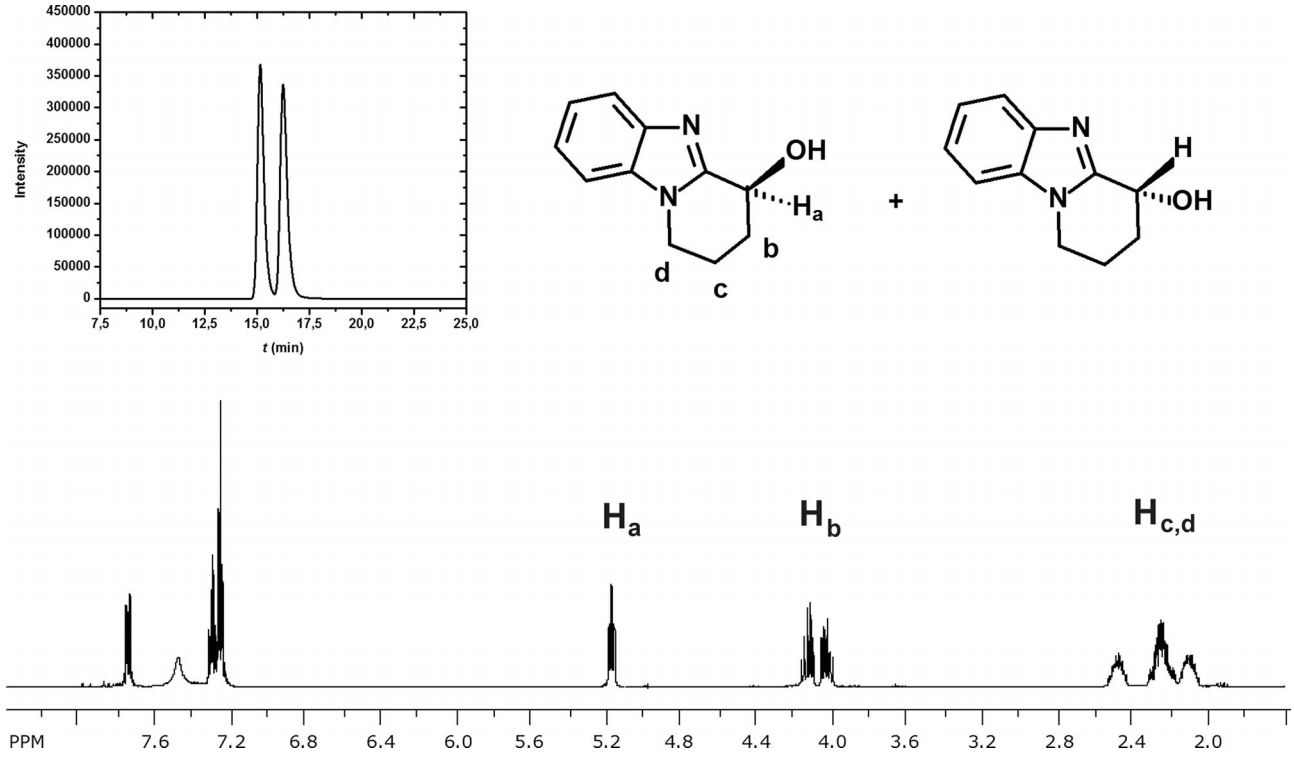

Figure 8. ^{1}H NMR spectroscopic analysis and HPLC chromatogram of both enantiomers of **6** obtained by using an analytical HPLC column with a chiral stationary phase [Chiralpak IC; *n*-heptane/CH_2Cl_2/EtOH:diethylamine (75:25:3:0.1); t_1 = 15.15 min, t_2 = 16.24 min; T = 25 °C; flow rate 1.0 mL/min].

planar, fused, six-membered ring. Moreover, the chlorine atom occupies the *trans*-position relative to the phosphorus atom, whereas the CO molecule is coordinated *trans* to the benzimidazole moiety.

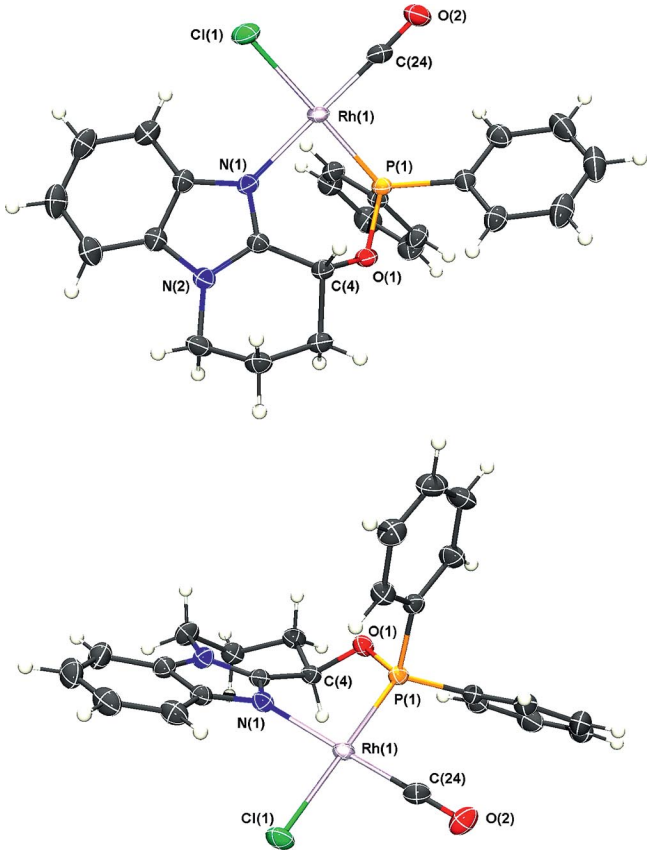

Figure 9. Molecular structure of **8** determined by X-ray crystal structure determination. Only one enantiomer of the racemic crystal structure is shown. Displacement ellipsoids are shown at the 50% probability level. Selected bond lengths (Å): Rh(1)–P(1): 2.1925(4); Rh(1)–N(1): 2.0982(12); P(1)–O(1): 1.6337(11); Rh(1)–Cl(1): 2.3897(4); Rh(1)–C(24): 1.8192(16); O(2)–C(24): 1.147(2); bond angle (°): P(1)–Rh(1)–N(1): 87.24(3).

Additional analysis revealed that complex **8** shows a doublet in the $^{31}P\{^{1}H\}$ NMR spectrum at δ = 132.8 ppm (J = 178.2 Hz) and a CO stretching frequency of $\tilde{\nu}$ = 1992 cm^{-1} in the IR spectrum. In comparison to imidazole-based Rh complexes analyzed by Field et al.,[14] ligand **7** has clearly more π-accepting characteristics than the reported phosphine-based ligands.

To gain further insight into the applicability of the newly developed P,N-ligand in homogeneous catalytic reactions, we performed iridium-catalyzed hydrogenation reactions of *N*-phenyl-(1-phenylethylidene)amine (**9**; Scheme 6) and *trans*-α-methylstilbene (**10**; Scheme 7) in a parallel reactor system (AMTEC SPR16). At 25 °C and a constant hydrogen pressure (10 bar), substrate **9** was quantitatively converted into the hydrogenated product **9a** within 16 h (TOF = 107 h^{-1} at 10% conversion).

From the gas uptake plot (Figure 10) it is clear that, within the first two hours, approximately 90% of **9** was converted into the product, which was followed by a sharp decrease in H_2 gas consumption towards the end of the reaction. Substrate **10** was hydrogenated under the same reaction conditions, although only half of the concentration of **9** was used. The gas uptake plot for **10** (Figure 11) showed a significantly reduced activity compared with **9**, which reached a conversion of 67% after 16 h (TOF = 20 h^{-1} at 10% conversion). Turnover frequencies were determined at 10% conversion because the reaction with substrate **10** was no longer in the linear regime.

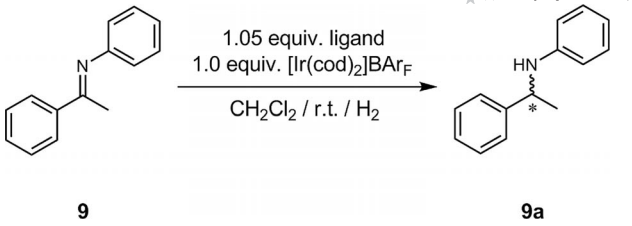

Scheme 6. Iridium-catalyzed hydrogenation of *N*-phenyl-(1-phenylethylidene)amine **9**. Reaction conditions: 25 °C, H_2 (10 bar), CH_2Cl_2, V_{tot} = 8.0 mL. Ir/L/S = 1:1.05:100. **9** (2.0 mmol), $[Ir(cod)_2]BAr_F$, $c_{Ir} = 1.6 \times 10^{-4}$ mol L^{-1}. Ligand = *rac*-**7** or **12**.

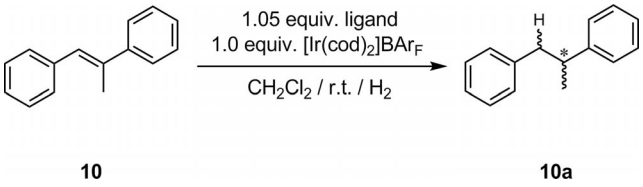

Scheme 7. Iridium-catalyzed hydrogenation of *trans*-α-methylstilbene **10**. Reaction conditions: 25 °C, H_2 (10 bar), CH_2Cl_2, V_{tot} = 8.0 mL. Ir/L/S = 1:1.05:50. **10** (1.0 mmol), $[Ir(cod)_2]BAr_F$, $c_{Ir} = 1.6 \times 10^{-4}$ mol L^{-1}. Ligand = *rac*-**7**. For ligand = **12**: Ir/L/S = 1:1.05:100.

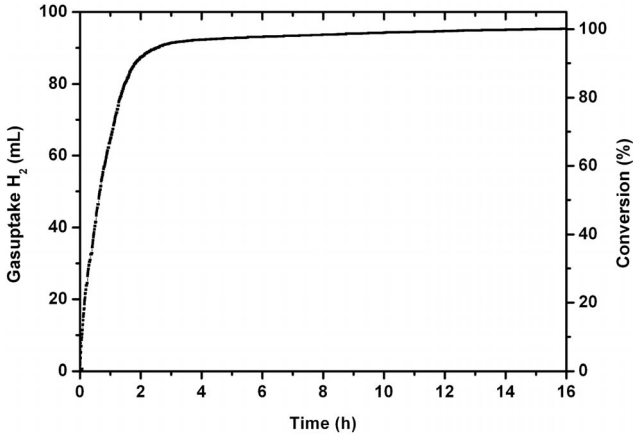

Figure 10. Gas uptake curve for the hydrogenation of **9** with *rac*-**7**/Ir^+.

Because the preparation of the P,N-hybrid ligand was successful and its coordination chemistry as well as its applicability in hydrogenation reactions had been explored, we then started to investigate the chiral resolution of the enantiomers so that enantiopure **7** could be applied as ligand in asymmetric catalytic reactions. To this end, *rac*-**6** was dissolved in a mixture of *n*-heptane/CH_2Cl_2/EtOH/di-

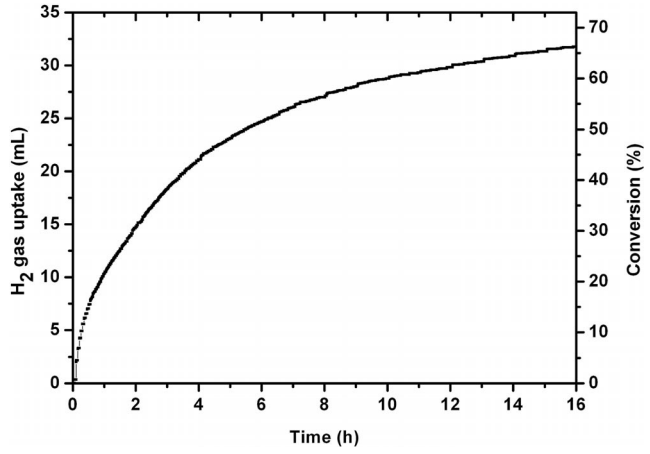

Figure 11. Gas uptake curve for the hydrogenation of **10** with *rac*-**7**/Ir^+.

ethylamine (75:25:3:0.1) and analyzed by means of chiral HPLC. Baseline separation of **6**-E_1 (first eluted enantiomer) and **6**-E_2 (second eluted enantiomer) was only achieved at low concentrations by using an analytical HPLC with a chiral stationary phase [Chiralpak IC; *n*-heptane/CH_2Cl_2/EtOH-diethylamine (75:25:3:0.1); t_1 = 15.15 min, t_2 = 16.24 min; T = 25 °C; flow rate: 1.0 mL/min; see also Figure 8]. With the separation of the two enantiomers by chiral HPLC achieved, we could obtain both fractions in high enantiopurity for further characterization.

To assign the absolute configurations of **6**-E_1 and **6**-E_2, the optical properties of the separated enantiomers were determined by circular dichroism (CD) in $ClCH_2CH_2Cl$; the experimentally recorded spectra are shown in Figure 12 (top).

The bisignate (–/+) CD curve of **6**-E_1 shows the presence of an exciton split couplet with a relatively small amplitude of $\Sigma\Delta\varepsilon \approx 10$, whereas the bisignate (+/–) CD curve of **6**-E_2 has a couplet with an amplitude of $\Sigma\Delta\varepsilon \approx 12$. The CD spectra also display two Cotton effects for each enantiomer at $\lambda \approx 290$ and 255 nm. The deviation in $\Sigma\Delta\varepsilon$ values between the two enantiomers can be attributed to a difference in concentration as a result of the enrichment procedure.

To deduce the absolute configuration, the CD spectra for both enantiomers were simulated by means of a time-dependent Density Functional Theory method at the B3LYP/6-311+G(d,p) level. This technique has been shown to provide a reasonably accurate description of the photophysical properties of various compounds, which include quite accurate predictions of CD spectra.[15] The geometries for (*R*)-**6** and (*S*)-**6** were optimized at the B3LYP/6-311+G(d,p) level and their theoretical CD spectra were calculated as shown in Figure 12 (bottom). The theoretical CD spectra of both enantiomers also display the same characteristic features as the experimentally obtained spectra. The calculated spectra clearly show the bisignate shape as well as the sequence of the negative/positive Cotton effects. Both the (–/+) pattern and the (+/–) pattern are clearly visible, however, the peaks show a redshift to higher wavelengths, and the intensity maxima and minima of the theoretical spectra are, in general, larger than those in the experimental spectra. For the theoretical calculations, both conformers were structurally optimized and although the rotation of the hydroxyl group as well as the fluxional chaired C_4H_7OH "bridge" have influence on the shape of the theoretical CD spectrum, the overall bisignate character as seen in the theoretical and the experimental spectra remains unchanged. Furthermore, the spectra are independent of the conformations of these side groups.

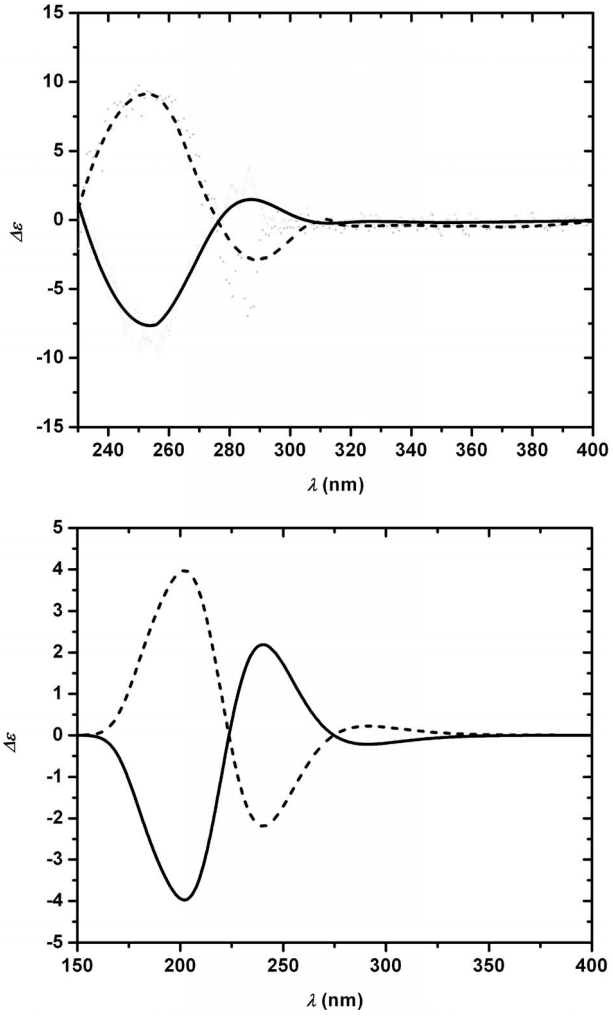

Figure 12. (Top) Experimental CD spectra of **6**-E_1 (solid line) and **6**-E_2 (dashed line) in $ClCH_2CH_2Cl$. The experimental CD spectra (gray dots) have been smoothed (dashed line) to reduce the high noise level. (Bottom) Theoretical CD spectra of enantiomers (*S*)-**6** (solid line) and (*R*)-**6** (dashed line).

By applying the Cahn–Ingold–Prelog priority rules,[16] the absolute configuration of both enantiomers could be determined. Because the calculated data are in such a close agreement with the experimental results, we are confident to assign unambiguously the (*S*)-**6** configuration to the **6**-E_1 enantiomer and the (*R*)-**6** configuration to the **6**-E_2 enantiomer (Figure 13).

Unfortunately, it turned out that at higher concentrations both peaks of **6** start to overlap significantly in the HPLC chromatogram, making separation on multimiligram scale

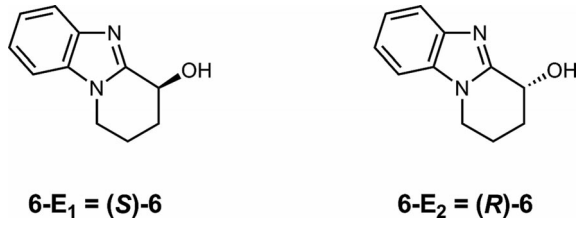

Figure 13. (Left) Enantiomer **6**-E_1 (first eluted compound) having the *S* configuration. (Right) Enantiomer **6**-E_2 (second eluted compound) having the *R* configuration.

very tedious and almost impossible. Therefore, the approach of separating the enantiomers of **6** on a larger scale by using semipreparative HPLC was abandoned and we shifted our focus to a different method. We chose the kinetic resolution of **6** by using a transesterification reaction catalyzed by *Candida Antarctica* lipase B (CALB) immobilized on acrylic resin (Novozym 435), and used vinyl butyrate as the acyl donor (Scheme 8). Lipases are the most widely investigated enzymes due to their ease of handling and because of their increased stability at high temperatures and over a wide pH range.[17] Moreover, lipases are specific towards the ester bond and, hence, the formation of undesirable byproducts is eliminated.[18] Novozym 435 has been applied in the synthesis of long-chain fatty acids and sugars, in the preparation of long-chain acyl thioesters,[19] and in the transesterification of several alcohols.[20]

The kinetic resolution of secondary alcohol **6** was investigated under different reaction conditions. Novozym 435 has been reported to be stable up to 90 °C, however, a temperature of 50 °C proved to be more efficient in our case. A combination of toluene as solvent and Novozym 435 (25 w/w-%) in the presence of vinyl butyrate (1.05 equiv.) gave the best results within 23 h, as indicated by HPLC and ^{1}H NMR analysis after optimization of the enzymatic kinetic resolution (Figure 14).

Ester (*R*)-**11** could easily be separated from alcohol (*S*)-**6** by column chromatography (Si; hexane/EtOAc, 1:1) and, after subsequent washing of the column with MeOH, alcohol (*S*)-**6** was isolated in pure form with an enantiomeric excess of more than 99% as determined by chiral HPLC analysis. The ^{1}H NMR spectrum of the ester product showed a downfield shift from 5.2 to 6.2 ppm for the proton located at the carbon atom connected to the hydroxyl group, which allowed for an accurate determination of the conversion for each reaction. HPLC analysis of the reaction mixture over time clearly showed that the (*R*)-

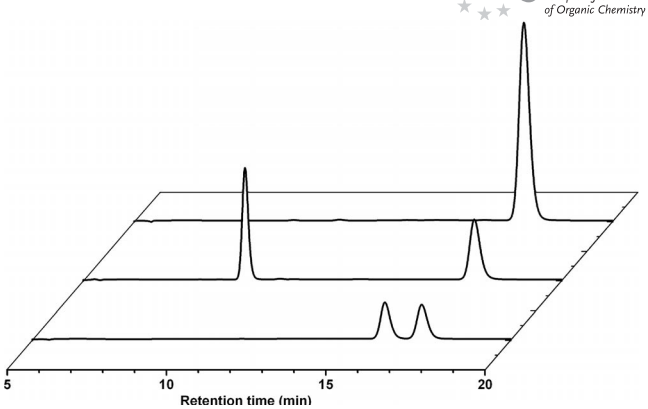

Figure 14. Front: HPLC analysis of baseline separation of both enantiomers of **6** by using analytical HPLC on a chiral stationary phase [Chiralpak IC; *n*-heptane/CH_2Cl_2/EtOH-diethylamine (75:25:3:0.1); t_1 = 16.06 min, t_2 = 17.21 min; T = 25 °C; flow rate: 1.0 mL/min). Middle: Transesterification reaction after 23 h; t_{ester} = 10.06 min and unreacted **6**-E_1. Background: First eluted enantiomer **6**-E_1 after column chromatography.

enantiomer had reacted completely towards the corresponding ester **11** and that only a fraction of the slower reacting (*S*)-enantiomer had also been converted. This reaction profile indicated that the enzymatic transesterification reaction followed Kazlauskas' rule.[21]

Ester (*R*)-**11** could easily be hydrolyzed to the corresponding alcohol (*R*)-**6** by stirring overnight in an aqueous methanolic solution (MeOH/H_2O, 4:1) in the presence of a ten-fold excess of K_2CO_3 (Scheme 9).

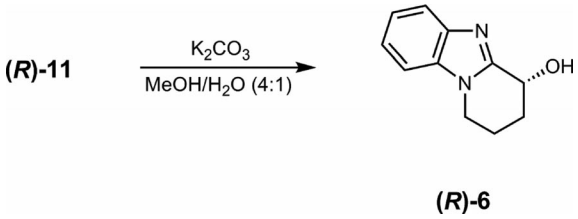

Scheme 9. Hydrolysis of ester (*R*)-**11** to alcohol (*R*)-**6**.

Chiral HPLC analysis indicated an enantiomeric excess of 96%. In subsequent reactions, as described in Scheme 4, both enantioenriched alcohols (*S*)-**6** (> 99% ee) and (*R*)-**6** (96% ee) were converted into their corresponding P,N-ligands, (*S*)-**12** and (*R*)-**12**, respectively (Figure 15).

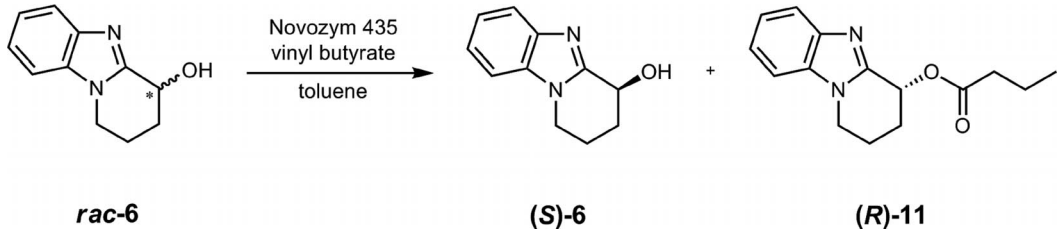

Scheme 8. Kinetic resolution of *rac*-**6** by using *Candida Antarctica* lipase B (Novozym 435) and vinyl butyrate as acyl donor.

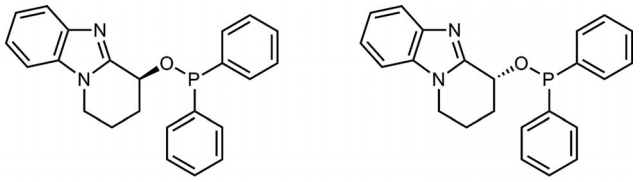

Figure 15. (Left) Bidentate P,N-ligand (*S*)-**12**. (Right) Bidentate P,N-ligand (*R*)-**12**.

To investigate the enantioselectivity and activity of the metal complexes based on the bidentate P,N-ligand **12**, *N*-phenyl-(1-phenylethylidene)amine (**9**; Scheme 6) and *trans*-α-methylstilbene (**10**; Scheme 7) were chosen as model substrates in the Ir-catalyzed asymmetric hydrogenation. The catalytic reactions with (*S*)-**12**/Ir^+ and (*R*)-**12**-*R*/Ir^+ were carried out by using a stainless steel 75-mL autoclave equipped with a dropping funnel. The autoclave was first charged with the iridium-based precatalyst solution followed by the substrate solution, filled with H_2 at the desired pressure, and sealed. The substrates were hydrogenated at 25 °C and H_2 (10 bar) for 20–24 h. From Table 1 it is clear that imine **9** is quantitatively hydrogenated within 24 h as determined by ^1H NMR spectroscopy (entries 1 and 2). Unfortunately, analysis of the reaction products by chiral HPLC revealed an enantiomeric excess of only 10% for both catalysts (*S*)-**12**/Ir^+ (*S* product) and (*R*)-**12**/Ir^+ (*R* product). However, applying olefin **10** in the asymmetric hydrogenation under the same conditions resulted in very good enantioselectivities for both catalysts (*S*)-**12**/Ir^+ and (*R*)-**12**/Ir^+ with enantiomeric excesses of 80 (*R* product) and 90% (*S* product), respectively (entries 3 and 4).

Table 1. Asymmetric hydrogenation of *N*-phenyl-(1-phenyl-ethylidene)amine and *trans*-α-methylstilbene.[a]

Entry	Ligand	Substrate	*p* [bar]	Conv. [%][b]	*ee* [%][e]
1	(*S*)-**12**	9	10	100[c]	10 (*S*)
2	(*R*)-**12**	9	10	100[c]	10 (*R*)
3	(*S*)-**12**	10	10	91[d]	80 (*R*)
4	(*R*)-**12**	10	10	>99[d]	90 (*S*)
5	(*R*)-**12**	10	5	59[d]	73 (*S*)
6	(*R*)-**12**	10	20	41[d]	82 (*S*)

[a] Reaction conditions: $[Ir(cod)_2]BAr_F$, Ir/L/S = 1:1.05:100, c_{Rh} = 2.5 mM, V_{tot} = 12 mL, CH_2Cl_2, 25 °C. [b] Conversion was determined by ^1H NMR spectroscopic analysis. [c] Determined after 24 h. [d] Determined after 20 h. [e] The *ee* was determined by analytical chiral HPLC.

Interestingly, these results clearly reveal that the less enantiopure catalyst (*R*)-**12**/Ir^+ (from (*R*)-**6**, having 96% *ee*) obtained from the enzymatic kinetic resolution of the chiral alcohol is slightly more enantioselective than (*S*)-**12**/Ir^+ (from (*S*)-**6**, having > 99% ee). During the workup, after the enzymatic kinetic resolution, only substantial amounts of the unreacted alcohol (*R*)-**6** could be eluted from the column by using pure MeOH. During this procedure, minute amounts of impurities could also be washed off the column, which could be the reason for the somewhat reduced enantioselectivity. Furthermore, it might also by possible that a small amount of enantiomeric purity could have been lost during the reaction from **6** to **12**. Table 1 also indicates that performing the reaction at reduced pressure (5 bar) or higher pressure (20 bar) both resulted in a significant reduction in conversion as well as a small decrease in enantioselectivity.

Conclusions

Our recently discovered tandem hydroformylation–cyclization sequence of *N*-allyl-substituted imidazole-derivatives towards OH-functionalized nitrogen heterocycles provides the possibility of synthesizing novel chiral P,N-ligands. Structure elucidation of the chiral ligand and the corresponding metal complexes by means of CD spectroscopy and X-ray crystal structure analysis provides valuable information on their absolute configuration and coordination behavior. Furthermore, the first enantiopure compound of this type has been successfully used in the enantioselective iridium-catalyzed hydrogenation of *N*-phenyl(1-phenylethylidene)amine and α-methylstilbene and enantiomeric excess values of up to 90% could be obtained. Interestingly, the modular synthetic procedure used for the preparation of the P,N-ligands provides the possibility to vary the substitution pattern of the ligand backbone in a facile way, so that a wide variety of substituted chiral P,N-ligands are easily accessible. The scope of the hydroformylation–cyclization sequence and the preparation of the corresponding chiral P,N-ligands as well as their application in asymmetric homogeneous catalysis is being explored in our laboratories.

Experimental Section

General: All manipulations were carried out under an argon atmosphere by using modified Schlenk techniques, unless stated otherwise. All glassware was dried prior to use by heating under vacuum. All common chemicals were commercially available and purchased from Aldrich Chemical Co., Merck or Strem Chemicals and used as received. α-Methylstilbene was purchased from Merck and used as received. *N*-Phenyl(1-phenylethylidene)amine was prepared according to a modified literature procedure.[5a] Solvents were dried and deoxygenated by using custom-made solvent purification columns filled with Al_2O_3. Elemental analyses were recorded by H. Kolbe, Mikroanalytisches Laboratorium, Mülheim a.d. Ruhr (Germany). ^1H, $^{13}C\{^1H\}$ and $^{31}P\{^1H\}$ NMR spectra were recorded with a Varian Mercury 400 spectrometer and all chemical shifts are reported relative to the residual proton resonance in the deuterated solvents or referred to an 85% aqueous solution of H_3PO_4, respectively.

***N*-(2-Methylallyl)benzimidazole (1):** Dimethyl sulfoxide (120 mL) was added to KOH (19.0 g, 338.6 mmol, 4.0 equiv.) and the mixture was stirred for 5 min, followed by the addition of benzimidazole (10.03 g, 84.8 mmol, 1.0 equiv.). The mixture was stirred for another 45 min, then cooled to a slurry using an ice-water bath. 3-Bromo-1-propene (11.26 g, 93.1 mmol, 1.1 equiv.) was added dropwise and stirring was continued for 2 h under ice cooling, and for a further 1.5 h without ice cooling. The reaction was quenched by the addition of water (300 mL) and the aqueous phase was extracted with CH_2Cl_2 (3 × 300 mL). The organic phase was back-

extracted with water (3 × 300 mL), dried with anhydrous Na_2SO_4, filtered, and all volatiles were removed in vacuo to give **1** (13.32 g, 77.3 mmol, 91.0%) as a white solid. ^{1}H NMR (400.16 MHz, $CDCl_3$, 25 °C): δ = 1.67 (s, 3 H, Me), 4.65 (s, 2 H, H_2C=C), 4.79 (br. s, 1 H), 4.96 (br. s, 1 H), 7.24–7.30 (m, 2 H), 7.32–7.38 (m, 1 H), 7.78–7.84 (m, 1 H), 7.86 (s, 1 H) ppm. ^{13}C NMR (100.62 MHz, $CDCl_3$, 25 °C): δ = 19.9, 51.1, 110.1, 114.3, 120.2, 122.2, 123.1, 134.3, 139.5, 143.3, 143.7 ppm. MS: *m*/*z* = 171.10 $[M]^+$.

2-Methyl-1,2,3,4-tetrahydrobenzo[4,5]imidazo[1,2-α]pyridin-4-ol (3): A 75-mL stainless steel autoclave equipped with a sampling unit and dropping funnel was charged with a solution of [Rh(acac)-$(CO)_2$] (2.1 mg, 8.0×10^{-6} mmol, 1.0 equiv.) and phosphabarrelene[8] (20 equiv.) in THF (5 mL). To the dropping funnel was added dropwise a solution of **1** (12.0 mmol, 1500 equiv.) in THF (1.5 mL). The autoclave was sealed and pressurized with CO/H_2 (1:1; 20 bar) and heated to preformation temperature and stirred for 2 h. Subsequently, the substrate was added by using the dropping funnel to the preformed catalyst solution initiating the start of the reaction. When the reaction was complete, the autoclave was cooled and the pressure was released. Crystallization from hot THF gave the product as colorless crystals or as a white powder.

Isomer *anti*-(*S*,*S*)-(3): ^{1}H NMR (400.16 MHz, $CDCl_3$, 25 °C): δ = 7.77–7.75 (m, 1 H), 7.35–7.25 (m, 3 H), 6.23 (br, 1 H), 5.25 (t, *J* = 3.5 Hz, 1 H), 4.29–4.24 (ddd, *J* = 11.9, 5.2, 0.8 Hz, 1 H), 3.55–3.49 (t, *J* = 11.3 Hz, 1 H), 2.82–2.78 (br, 1 H), 2.34–2.30 (m, 1 H), 1.90–1.82 (ddd, *J* = 14.0, 12.0, 4.1 Hz, 1 H), 1.25–1.23 (d, *J* = 6.7 Hz, 3 H) ppm. ^{13}C NMR (100.62 MHz, $CDCl_3$, 25 °C): δ = 153.52, 142.25, 133.77, 122.44, 122.37, 119.19, 109.38, 61.14, 49.20, 37.58, 23.94, 18.71 ppm. MS: *m*/*z* = 201.11 $[M]^+$.

Isomer *syn*-(*S*,*R*)-(3): ^{1}H NMR (400.16 MHz, $CDCl_3$, 25 °C): δ = 7.77–7.75 (m, 1 H), 7.35–7.25 (m, 3 H), 5.98 (br, 1 H), 5.08 (dd, *J* = 11.0, 6.3 Hz, 1 H), 4.21–4.16 (ddd, *J* = 11.4, 5.2, 1.1 Hz, 1 H), 3.56–3.50 (t, *J* = 11.4 Hz, 1 H), 2.51–2.46 (m, 1 H), 2.36–2.29 (m, 1 H), 1.81–1.72 (dt, *J* = 12.6, 11.2 Hz, 1 H), 1.27–1.25 (d, *J* = 6.7 Hz, 3 H) ppm. ^{13}C NMR (100.62 MHz, $CDCl_3$, 25 °C): δ = 155.22, 142.64, 133.93, 122.44, 122.37, 119.19, 109.38, 63.98, 49.07, 38.65, 28.01, 18.89 ppm. MS: *m*/*z* = 201.11 $[M]^+$. $C_{12}H_{14}N_2O$ (202.25): calcd. C 71.26, H 6.98, N 13.85; found C 72.93, H 7.48, N 13.13.

X-ray Crystal Structure Determination: X-ray intensities were measured with a Nonius KappaCCD diffractometer with a rotating anode (compound **3**) or with a Bruker Kappa ApexII diffractometer with sealed tube (compound **8**) at a temperature of 150(2) K. The intensities were integrated by using Eval15[22] (compound **3**) or Saint[23] (compound **8**). Absorption correction and scaling was performed with SADABS.[24] The structures were solved by Direct Methods with the program SHELXS-97.[25] Least-squares refinement was performed with SHELXL-97[25] against F^2 of all reflections. Non-hydrogen atoms were refined with anisotropic displacement parameters. All hydrogen atoms were located in difference Fourier maps. The OH hydrogen atom in **3** was refined freely with an isotropic displacement parameter, all other hydrogen atoms were refined by using a riding model. Geometry calculations and checking for higher symmetry was performed with the PLATON program.[26]

CCDC-948396 (for **3**) and -948397 (for **8**) contain the supplementary crystallographic data for this paper. These data can be obtained free of charge from The Cambridge Crystallographic Data Centre via www.ccdc.cam.ac.uk/data_request/cif.

Compound 3: $C_{12}H_{14}N_2O$; F_w = 202.25; colorless plate; $0.42 \times 0.24 \times 0.12$ mm^3; triclinic; $P\bar{1}$ (no. 2); *a* = 6.39757(16), *b* = 8.2853(2), *c* = 10.3507(3) Å, α = 82.022(1), β = 77.139(1), γ = 79.627(1)°; *V* = 523.35(2) Å^3; λ = 0.71073 Å; *Z* = 2; D_x = 1.283 g cm^{-3}; μ = 0.08 mm^{-1}. 9024 Reflections were measured up to a resolution of $(\sin\theta/\lambda)_{max}$ = 0.65 Å^{-1}. 2400 Reflections were unique (R_{int} = 0.029), of which 2022 were observed [$I > 2\sigma(I)$]. 141 Parameters were refined with no restraints. R_1/wR_2 [$I > 2\sigma(I)$]: 0.0428/0.1114. R_1/wR_2 [all refl.]: 0.0515/0.1177. *S* = 1.036. Residual electron density between –0.21 and 0.28 e Å^{-3}.

Compound 8: $C_{24}H_{21}ClN_2O_2PRh$; F_w = 538.76; yellow needle; $0.25 \times 0.12 \times 0.09$ mm^3; triclinic; $P\bar{1}$ (no. 2); *a* = 10.1357(3), *b* = 11.4360(3), *c* = 12.0375(4) Å, α = 62.2554(7), β = 65.1659(7), γ = 69.0578(7)°; *V* = 1097.68(6) Å^3; λ = 0.71073 Å; *Z* = 2; D_x = 1.630 g cm^{-3}; μ = 1.00 mm^{-1}. 23385 Reflections were measured up to a resolution of $(\sin\theta/\lambda)_{max}$ = 0.65 Å-1. 5015 Reflections were unique (R_{int} = 0.016), of which 4679 were observed [$I > 2\sigma(I)$]. 280 Parameters were refined with no restraints. R_1/wR_2 [$I > 2\sigma(I)$]: 0.0189/0.0485. R_1/wR_2 [all refl.]: 0.0213/0.0497. *S* = 1.037. Residual electron density between –0.25 and 0.43 e Å^{-3}.

1-Allylbenzimidazole (4): A mixture of DMSO (120 mL) and KOH pellets (19.0 g, 338.6 mmol, 4.0 equiv.) was stirred for 5 min, then benzimidazole (10.0 g, 84.6 mmol, 1.0 equiv.) was added and stirring was continued for 45 min. The mixture was ice-cooled to a slurry and allyl bromide (11.3 g, 93.4 mmol, 1.1 equiv.) was added dropwise. The ice bath was removed and the stirring was continued for 45 min, then the mixture was poured onto ice-cooled water (100 mL) and stirred for a further 30 min. The aqueous phase was extracted with diethyl ether (3 × 100 mL) and the organic phase was back-extracted with water (3 × 100 mL), dried with anhydrous $MgSO_4$, filtered, and all volatiles were removed in vacuo to give **4** (10.1 g, 63.8 mmol, 75%) as a pale-yellow oil. ^{1}H NMR (400 MHz, $CDCl_3$, 25 °C): δ = 4.67–4.70 (dq, *J* = 5.5, 1.4 Hz, 2 H), 5.09–5.26 (m, 2 H), 5.88–5.98 (m, 1 H), 7.22–7.27 (m, 2 H), 7.29–7.34 (m, 1 H), 7.77–7.81 (m, 1 H), 7.83 (s, 1 H) ppm. ^{13}C NMR (100.63 MHz, $CDCl_3$, 25 °C): δ = 47.4, 109.9, 118.6, 120.3, 122.2, 122.7, 131.9, 133.6, 142.9, 143.6 ppm; $C_{10}H_{10}N_2$ (158.20): calcd. C 75.92, H 6.37, N 17.71; found C 74.50 H 6.59 N 17.54.

1,2,3,4-Tetrahydrobenzo[4,5]imidazo[1,2-*a*]pyridin-4-ol (6): To a mixture of [Rh(acac)$(CO)_2$] (5.4 mg, 2.1×10^{-2} mmol, 1.0 equiv.) and Xantphos (48.8 mg, 8.4×10^{-2} mmol, 4 equiv.) was added toluene (13 mL). The reaction mixture was stirred for 15 min and transferred to a 75-mL stainless steel autoclave also equipped with a dropping funnel. A mixture of **4** (5.0 g, 31.6 mmol, 1500 equiv.) and toluene (4 mL) was added to the dropping funnel and the catalyst solution was preformed at 140 °C and 20 bar (CO/H_2) for 2 h. After preformation, the substrate solution was added to the catalyst solution by using the dropping funnel, which initiated the start of the reaction. After 72 h, the autoclave was cooled and the pressure was released. The reaction mixture was purified by flash column chromatography (silica; *n*-hexane/EtOAc, 1:1, followed by MeOH) to give the crude product mixture. Crystallization from a minimal amount of toluene gave the **6** (2.26 g, 12.0 mmol, 38%) as colorless crystals or as a white powder, m.p. 172 °C. ^{1}H NMR (400.16 MHz, $CDCl_3$, 25 °C): δ = 2.04–2.14 (m, 1 H, CH_2 next to chiral carbon), 2.16–2.32 (m, 2 H, CH_2), 2.42–2.52 (m, 1 H, CH_2 next to chiral carbon), 3.99–4.16 (m, 2 H, CH_2N), 5.17 (t, *J* = 5.6 Hz, 1 H, H on the chiral carbon atom), 7.24–7.33 (m, 3 H), 7.49 (br. s, 1 H, –OH, position may vary), 7.73–7.78 (m, 1 H) ppm. ^{13}C NMR (100.63 MHz, $CDCl_3$, 25 °C): δ = 18.99, 29.57, 42.51, 62.30, 109.46, 119.09, 122.47 (2C), 133.96, 142.04, 154.45 ppm. $C_{11}H_{12}N_2O$ (188.23): C 70.19, H 6.43, N 14.88; found C 69.00, H 6.60, N 14.90.

4-[(Diphenylphosphanyl)oxy]-1,2,3,4-tetrahydrobenzimidazo[1,2-*a*]-pyridine (7): A mixture of **6** (513.8 mg, 2.73 mmol, 1.0 equiv.), tri-

ethylamine (690.5 mg, 6.83 mmol, 2.5 equiv.) and dichloromethane (10 mL) under an argon atmosphere was cooled to –78 °C and subsequently chlorodiphenylphosphine (602.2 mg, 2.73 mmol, 1.0 equiv.) in dichloromethane (3 mL) was added dropwise. The mixture was warmed to room temperature overnight, then all volatiles were removed in vacuo. The crude reaction mixture was redissolved in toluene and the triethylammonium chloride was filtered off, washed with toluene and concentrated to give **7** (911.5 mg, 2.45 mmol, 90%) as a white solid. ^{1}H NMR (400.16 MHz, $CDCl_3$, 25 °C): δ = 1.99–2.12 (m, 2 H), 2.29–2.51 (m, 2 H), 3.89–4.26 (m, 2 H, CH_2N), 5.35–5.39 (m, 1 H, H on the chiral carbon atom), 7.14–7.60 (m, 11 H), 7.56–7.60 (m, 2 H), 7.79–7.83 (m, 1 H) ppm. ^{13}C NMR (100.62 MHz, $CDCl_3$, 25 °C): δ = 18.07, 29.25, 29.30, 42.43, 42.61, 71.44, 71.67, 119.83, 122.14, 122.43, 127.99, 128.06, 128.25, 128.32, 128.85, 129.42, 129.81, 130.02, 130.39, 130.62, 142.08, 142.25, 142.51, 142.70, 142.90, 150.24, 150.31 ppm. ^{31}P NMR (161.98 MHz, $CDCl_3$, 25 °C): δ = 114.6 ppm. $C_{23}H_{21}N_2OP$ (372.40): C 74.18, H 5.68, N 7.52; found C 73.77, H 5.67, N 7.27.

[(4)Rh(CO)Cl] (8): A solution of **7** (25.0 mg, 0.067 mmol, 1.0 equiv.) in CH_2Cl_2 (4 mL) was added dropwise under argon to a solution of μ-dichlorotetracarbonyldirhodium (13.0 mg, 0.034 mmol, 0.5 equiv.) in CH_2Cl_2 (4 mL). Upon addition the solution became bright-yellow and CO formation was observed. The mixture was stirred for 1 h at r.t., then all volatiles were removed in vacuo to give complex **8** (36.1 mg, 0.067 mmol, quant.) as a yellow solid. ^{1}H NMR (400.16 Hz, CD_2Cl_2, 25 °C): δ = 2.03–2.15 (m, 2 H), 2.26–2.35 (m, 1 H), 2.46–2.57 (m, 1 H), 3.98–4.37 (m, 2 H), 5.30–5.32 (t, J = 3.6 Hz, 1 H), 7.43–7.53 (m, 11 H), 7.69–7.82 (m, 2 H), 7.99–8.01 (m, 1 H) ppm. ^{13}C NMR (100.62 MHz, CD_2Cl_2, 25 °C): δ = 20.04, 28.39, 28.48, 43.31, 70.83, 110.59, 121.86, 124.09, 124.80, 128.74 (d, J = 11.7 Hz), 128.92 (d, J = 11.1 Hz), 131.58, 131.72, 131.85 (d, J = 1.8 Hz), 132.29, 132.44, 133.70, 135.84, 136.46, 138.03 (d, J = 4.6 Hz), 138.60 (d, J = 4.6 Hz), 140.12, 149.67 (d, J = 7.1 Hz), 189.04 (dd, $^1J_{Rh,C}$ = 72.3 Hz, $^2J_{P,C}$ = 17.5 Hz, *C*O) ppm. ^{31}P NMR (161.98 MHz, CD_2Cl_2, 25 °C): δ = 132.76 (d, $^1J_{Rh,P}$ = 178.2 Hz). IR (KBr): $\tilde{\nu}$ = 1992.12 cm^{-1}.

***N*-Phenyl(1-phenylethylidene)amine (9):** To molecular sieves (4 Å, 50 g) under argon was added toluene (60 mL), acetophenone (12.0 g, 100.0 mmol, 1.0 equiv.) and aniline (11.20 g, 120.0 mmol, 1.2 equiv.). The reaction mixture was heated to reflux for 48 h and subsequently cooled to room temperature. The molecular sieves were filtered off and all volatiles were removed on a rotavap and the residual liquid was distilled under high vacuum (b.p. 125 °C/0.04 mbar) affording **9** (17.11 g, 87.6 mmol, 88%) as a pale-yellow solid, m.p. 39 °C. ^{1}H NMR (400.16 MHz, $CDCl_3$, 25 °C): δ = 2.24 (s, 3 H), 6.78–6.83 (m, 2 H), 7.06–7.12 (m, 1 H), 7.33–7.38 (m, 2 H), 7.42–7.48 (m, 3 H), 7.95–8.01 (m, 2 H) ppm. ^{13}C NMR (100.62 MHz, $CDCl_3$, 25 °C): δ = 17.47, 119.47 (2C), 123.31, 127.27 (2C), 128.47 (2C), 129.05 (2C), 130.55, 139.58, 151.79, 165.55 ppm.

General Procedure for the Enzymatic Kinetic Resolution of 6: A mixture of Novozym 435 (482.5 mg, 25 w/w-%) and **6** (1.93 g, 10.25 mmol, 1 equiv.) in toluene (29 mL) was heated to 50 °C. Subsequently, vinyl butyrate (1.23 g, 10.77 mmol, 1.05 equiv.) was added dropwise and the mixture was stirred for 23 h. When the reaction was complete, the enzyme beads were filtered off and all volatiles were removed in vacuo. The ester was separated from the unreacted alcohol by column chromatography (silica; *n*-hexane/EtOAc, 1:1) to give ester (*R*)-**11** (916.7 mg, 3.55 mmol, 35%) as a white solid. The unreacted alcohol was washed from the column with pure MeOH to give alcohol (*S*)-**6** (417.9 mg, 2.22 mmol, 22%) as a white solid (> 99% ee). The enantiomeric excess of the alcohol was determined by chiral HPLC analysis.

(*R*)-1,2,3,4-Tetrahydrobenzo[4,5]imidazo[1,2-*a*]pyridin-4-yl Butyrate (11): M.p. 63 °C. ^{1}H NMR (400.16 MHz, $CDCl_3$, 25 °C): δ = 0.77 (t, J = 7.4 Hz, 3 H), 1.49 (q, J = 7.2 Hz, 2 H), 1.79–1.89 (m, 1 H), 1.91–1.98 (m, 2 H), 2.00–2.10 (m, 1 H), 2.16 (dt, J = 7.4, 2.9 Hz, 2 H), 2.62–2.72 (m, 1 H), 3.84–3.92 (m, 1 H), 5.98 (t, J = 4.7 Hz, 1 H), 7.00–7.10 (m, 3 H), 7.56–7.62 (m, 1 H) ppm. ^{13}C NMR (100.62 MHz, $CDCl_3$, 25 °C): δ = 13.14, 17.87, 18.05, 26.70, 35.62, 41.73, 64.39, 109.01, 119.35, 122.09, 122.32, 133.64, 142.06, 147.86, 171.78 ppm. $C_{15}H_{18}N_2O_2$ (258.32): C 69.74, H 7.02, N 10.84; found C 69.73, H 7.03, N 10.83.

Deprotection of (*R*)-11: A solution of (*R*)-**11** (605.4 mg, 2.3 mmol, 1.0 equiv.) and K_2CO_3 (3.21 g, 23.2 mmol, 10.0 equiv.) in MeOH/H_2O (20 mL, 4:1) was stirred for 20 h at room temperature. The crude alcohol was filtered through a short pad of silica, washed with MeOH, and subsequently dried with $MgSO_4$, filtered, and concentrated to give alcohol (*R*)-**6** (397.0 mg, 2.11 mmol, 92%) as a white solid (96% ee). The enantiomeric excess of the alcohol was determined by chiral HPLC analysis.

HPLC Analysis: HPLC analysis and fraction collection were performed with a Shimadzu LC-20AD pump, a Shimadzu SPD-20A prominence UV/Vis detector, a Shimadzu SIL-20A HT prominence autosampler, and a CTO-20AC prominence column oven. Column and analysis specifications for the one-pot tandem hydroformylation–cyclization sequence: Chiralcel OJ-H (250 × 4.6 mm, particle size: 5 μm, purchased from Daicel), eluent: *n*-hexane/2-propanol (98:2), column temperature: 25 °C, flow rate: 1.0 mL/min, p = 39 bar, λ = 254 nm (UV detector), injection volume: 20 μL. Column and analysis specifications for the enzymatic kinetic resolution: Chiralpak IC (250 × 4.6 mm, particle size: 5 μm, purchased from Daicel), eluent: *n*-heptane/CH_2Cl_2/EtOH/diethylamine (75:25:3:0.1), column temperature: 25 °C, flow rate: 1.0 mL/min, p = 28 bar, λ = 254 nm (UV detector), injection volume: 5 μL. Column and analysis specifications for the iridium-catalyzed hydrogenation reactions: Chiralcel OJ-H (250 × 4.6 mm, particle size: 5 μm, purchased from Daicel), eluent: *n*-hexane/2-propanol (99:1), column temperature: 25 °C, flow rate: 1.0 mL/min, p = 37 bar, λ = 254 nm (UV detector), injection volume: 3 μL.

CD Analysis: CD spectroscopic measurements were performed at 25 °C with a Jasco J-815 spectropolarimeter. Appropriate settings were chosen for the sensitivity, time constant, and scan rate, and 10.00 mm cuvettes were used. Racemate **6** (10.0 mg, 5.3×10^{-5} mol) was dissolved in a mixture of *n*-heptane/CH_2Cl_2/EtOH/diethylamine (75:25:3:0.1, 1.5 mL) prior to HPLC separation. Enantiomers **6**-E_1 and **6**-E_2 were eluted [eluent: *n*-heptane/CH_2Cl_2/EtOH/diethylamine (75:25:3:0.1)], collected and all volatiles were removed in vacuo. This procedure was performed five times and the combined residues of **6**-E_1 and **6**-E_2 were each redissolved in $ClCH_2CH_2Cl$ (1.5 mL) and diluted to give final concentrations of approximately 10^{-6} M. The CD spectra were recorded immediately.

Computational Details: Quantum chemical calculations were carried out by using Density Functional Theory (DFT) with the Gaussian 09 suite of programs.[27] All calculations were performed at the B3LYP/6-311G+(d,p) level of theory. Full geometry optimizations were done for compounds (*R*)-**6** and (*S*)-**6**. The nature of the stationary points was tested by analyzing the analytically calculated harmonic normal modes. All structures were confirmed to contain no imaginary frequencies. Theoretical CD spectra were calculated by using the time-dependent DFT (TD-DFT) method as implemented in the Gaussian 09 program.[27] The number of states included in the TD-DFT calculations was set to 50. The CD spectra were simulated by overlapping Gaussian functions for each transition; the width of the band at half height was fixed at 0.8 eV.

General Procedure for the Hydrogenation Experiments in a Stainless Steel Autoclave (75 mL): A solution of **12** (11.7 mg, 3.2×10^{-2} mmol, 1.05 equiv.) in CH_2Cl_2 (3.0 mL) was added dropwise at room temperature to a solution of $[Ir(cod)_2]BAr_F$ (38.2 mg, 3.0×10^{-2} mmol, 1.0 equiv.) in CH_2Cl_2 (3.0 mL), stirred for overnight and subsequently transferred to the 75-mL stainless steel autoclave. A solution of substrate **9** or **10** (3.0 mmol, 100 equiv.) in CH_2Cl_2 (6 mL) was added and the autoclave was sealed and filled with hydrogen gas. When the reaction was complete, excess H_2 pressure was released, the reaction mixture was filtered through a short pad of silica, and all volatiles were removed in vacuo. The conversions were determined by ^1H NMR analysis and the enantiomeric excess was determined by chiral HPLC: For the hydrogenation product of *N*-phenyl-(1-phenylethylidene)amine[28] (**9a**): Chiralcel OJ-H, *n*-hexane/2-propanol (99:1), t_R = 31.7 min, t_S = 40.7 min, $t_{substrate}$ = 36.3 min. The absolute configuration was determined by comparison of the optical rotation with literature.[5a] For the hydrogenation product of *trans*-α-methylstilbene (**10a**): Chiral HPLC:[29] Chiralcel OJ-H, *n*-hexane/2-propanol (99:1), t_S = 6.3 min, t_R = 8.5 min, $t_{substrate}$ = 13.7 min. Absolute stereochemistry was determined by comparison of the HPLC trace with that of the product obtained from hydrogenation of *trans*-α-methylstilbene with a known catalyst.[5b]

Reaction in an AMTEC Slurry-Phase Reactor SPR16 Parallel Reactor System: Catalysis experiments were performed in a parallel autoclave system AMTEC SPR16,[30] equipped with pressure sensors and a mass-flow controller suitable for monitoring and recording gas uptakes throughout the reaction.

General Procedure for the Catalysis Experiments: A stainless steel autoclave of the AMTEC SPR16 was heated to 90 °C and flushed with argon (15 bar) four times. Subsequently, the reactor was cooled to room temperature and flushing with argon was repeated again four times. The reactor was charged with a solution of the precatalyst in CH_2Cl_2 (4 mL, see below) as well as the substrate solution under argon (CH_2Cl_2, 4 mL, see below). The atmosphere was further exchanged with hydrogen gas and the reactor was pressurized with hydrogen to 3 bar. After heating to the desired temperature, the final pressure was adjusted and kept constant throughout the experiment. The gas uptake of hydrogen was monitored and recorded automatically. At the end of the catalysis experiments, the reactor was cooled to room temperature and the contents of the autoclave was filtered through a short pad of silica, all volatiles were removed in vacuo, and analyzed by means of ^1H NMR and HPLC. *Preparation of the precatalyst*: A solution of *rac*-**7** (7.8 mg, 2.1×10^{-2} mmol, 1.05 equiv.) in CH_2Cl_2 (2.0 mL) was added dropwise at room temperature to a solution of $[Ir(cod)_2]BAr_F$ (25.4 mg, 2.0×10^{-2} mmol, 1.0 equiv.) in CH_2Cl_2 (2.0 mL), stirred for 2 h and subsequently transferred to the 15 mL stainless steel autoclave. *Substrate solutions*: **9** (2.0 mmol, 100 equiv.) in CH_2Cl_2 (4 mL) or **10** (1.0 mmol, 50 equiv.) in CH_2Cl_2 (4 mL).

Hydrogenation Product of *N*-Phenyl-(1-phenylethylidene)amine[28] (9a): ^1H NMR (400.16 MHz, $CDCl_3$, 25 °C): δ = 1.54 (d, J = 6.8 Hz, 3 H), 4.24 (br. s, 1 H), 4.50 (q, J = 6.8 Hz, 1 H), 6.51–6.57 (m, 2 H), 6.66 (tt, J = 7.4, 1.0 Hz, 1 H), 7.08–7.10 (m, 2 H), 7.21–7.26 (m, 1 H), 7.30–7.35 (m, 2 H), 7.36–7.40 (m, 2 H) ppm; HPLC: Chiralcel OJ-H, *n*-hexane/2-propanol (99:1), t_R = 31.7 min, t_S = 40.7 min, $t_{substrate}$ = 36.3 min.

Hydrogenation Product of *trans*-α-Methylstilbene (10a): ^1H NMR (400.16 MHz, $CDCl_3$, 25 °C): δ = 1.26–1.24 (d, J = 6.8 Hz, 3 H), 2.15–2.80 (m, 1 H), 2.93–3.05 (m, 2 H), 7.08–7.10 (d, J = 7.2 Hz, 2 H), 7.17–7.30 (m, 8 H) ppm; Chiral HPLC:[29] Chiralcel OJ-H, *n*-hexane/2-propanol (99:1), t_S = 6.3 min, t_R = 8.5 min, $t_{substrate}$ = 13.7 min.

Supporting Information (see footnote on the first page of this article): ^1H, ^{13}C, and ^{31}P NMR spectra, IR spectra, HPLC traces from catalytic experiments.

Acknowledgments

The authors would like to thank Ing. Ton Staring (TU/e, Laboratory for Catalysis and Organometallic Chemistry) for technical assistance with the HPLC equipment. Dr. Anja Palmans (TU/e, department of Macromolecular and Organic Chemistry) is kindly acknowledged for a generous gift of Novozym 435. C. M. thanks The Netherlands Organization for Scientific Research (NWO-CW) for a personal grant (NWO Vidi and NWO Echo). The X-ray diffractometers were financed by NWO-CW.

[1] a) R. Noyori, in: *Asymmetric Catalysis in Organic Synthesis* Wiley-VCH, New York, **1994**, p. 16–94; b) H. Tayaka, T. Ohta, R. Noyori, in: *Catalytic Asymmetric Synthesis* (Ed.: I. Ojima), Wiley-VCH, New York, **1993**, p. 1–39; c) R. Noyori, *Angew. Chem.* **2002**, *114*, 2108–2123; *Angew. Chem. Int. Ed.* **2002**, *41*, 2008–2022; d) W. S. Knowles, *Angew. Chem.* **2002**, *114*, 2096–2107; *Angew. Chem. Int. Ed.* **2002**, *41*, 1998–2007; e) H.-U. Blaser, C. Malan, B. Pugin, F. Spindler, H. Steiner, M. Studer, *Adv. Synth. Catal.* **2003**, *345*, 103–151.

[2] See, for instance: a) *The Handbook of Homogeneous Hydrogenation* (Eds.: J. G. de Vries, C. J. Elsevier), Wiley-VCH, Weinheim, Germany, **2007**; b) P. W. N. M. van Leeuwen, in: *Homogeneous Catalysis – Understanding the Art*, Kluwer, Dordrecht, The Netherlands, **2004**, chapter 4, p. 75–100.

[3] a) R. L. Halterman, K. P. C. Vollhardt, M. E. Welker, D. Bläser, R. Boese, *J. Am. Chem. Soc.* **1987**, *109*, 8105–8107; b) V. P. Conticello, L. Brard, M. A. Giardello, Y. Tsuji, M. Sabat, C. L. Stern, T. J. Marks, *J. Am. Chem. Soc.* **1992**, *114*, 2761–2762; c) R. D. Broene, S. L. Buchwald, *J. Am. Chem. Soc.* **1993**, *115*, 12569–12570; d) M. A. Giardello, V. P. Conticello, L. Brard, M. R. Gagné, T. J. Marks, *J. Am. Chem. Soc.* **1994**, *116*, 10241–10254; e) M. V. Troutman, D. H. Appella, S. L. Buchwald, *J. Am. Chem. Soc.* **1999**, *121*, 4916–4917.

[4] R. Crabtree, *Acc. Chem. Res.* **1979**, *12*, 331–337.

[5] a) P. Schnider, G. Koch, R. Prétôt, G. Wang, F. M. Bohnen, C. Krüger, A. Pfaltz, *Chem. Eur. J.* **1997**, *3*, 887–892; b) A. Lightfoot, P. Schnider, A. Pfaltz, *Angew. Chem.* **1998**, *110*, 3047–3050; *Angew. Chem. Int. Ed.* **1998**, *37*, 2897–2899; c) P. G. Cozzi, N. Zimmermann, R. Hilgraf, S. Schaffner, A. Pfaltz, *Adv. Synth. Catal.* **2001**, *343*, 450–454; d) J. Blankenstein, A. Pfaltz, *Angew. Chem.* **2001**, *113*, 4577–4579; *Angew. Chem. Int. Ed.* **2001**, *40*, 4445–4447; e) F. Menges, A. Pfaltz, *Adv. Synth. Catal.* **2002**, *344*, 40–44; f) A. Pfaltz, J. Blankenstein, R. Hilgraf, E. Hörmann, S. McIntyre, F. Menges, M. Schönleber, S. P. Smidt, B. Wüstenberg, N. Zimmermann, *Adv. Synth. Catal.* **2003**, *345*, 33–43.

[6] a) D.-R. Hou, J. H. Reibenspiess, K. Burgess, *J. Org. Chem.* **2001**, *66*, 206–215; b) D.-R. Hou, J. H. Reibenspiess, T. A. Colacot, K. Burgess, *Chem. Eur. J.* **2001**, *7*, 5391–5400; c) M. T. Powell, D.-R. Hou, M. C. Perry, X. Cui, K. Burgess, *J. Am. Chem. Soc.* **2001**, *123*, 8878–8879; d) M. C. Perry, X. Cui, M. T. Powell, D.-R. Hou, J. H. Reibenspies, K. Burgess, *J. Am. Chem. Soc.* **2003**, *125*, 113–123; e) Y. Zhu, K. Burgess, *Acc. Chem. Res.* **2012**, *45*, 1623–1636.

[7] a) M. Engman, J. S. Diesen, A. Paptchikhine, P. G. Andersson, *J. Am. Chem. Soc.* **2007**, *129*, 4536–4537; b) P. Cheruku, A. Paptchikhine, T. L. Church, P. G. Andersson, *J. Am. Chem. Soc.* **2009**, *131*, 8285–8289; c) J. Mazuela, A. Paptchikhine, P. Tolstoy, O. Pàmies, M. Diéguez, P. G. Andersson, *Chem. Eur. J.* **2010**, *16*, 620–638.

[8] See, for instance: a) G. Jones, C. J. Richards, *Tetrahedron Lett.* **2001**, *42*, 5553–5555; b) G. Xu, S. R. Gilbertson, *Tetrahedron Lett.* **2003**, *44*, 953–955.
[9] N. Mršić, A. J. Minnard, B. L. Feringa, J. G. de Vries, *J. Am. Chem. Soc.* **2009**, *131*, 8358–8359.
[10] a) P. S. Bäuerlein, I. Arenas Gonzalez, J. J. M. Weemers, M. Lutz, A. L. Spek, D. Vogt, C. Müller, *Chem. Commun.* **2009**, 4944–4946; b) C. Müller, E. A. Pidko, D. Totev, M. Lutz, A. L. Spek, R. A. van Santen, D. Vogt, *Dalton Trans.* **2007**, 5372–5375.
[11] M. Kranenburg, Y. E. M. van der Burgt, P. C. J. Kamer, P. W. N. M. van Leeuwen, *Organometallics* **1995**, *14*, 3081–3089.
[12] a) M. J. Zacuto, F. Xu, *J. Org. Chem.* **2007**, *72*, 6298–6300; b) S. Krompiec, M. Krompiec, R. Penczek, H. Ignasiak, *Coord. Chem. Rev.* **2008**, *252*, 1819–1841.
[13] a) K. Hiraki, T. Matsunaga, H. Kawano, *Organometallics* **1994**, *13*, 1878–1885; b) S. Krompiec, N. Kúznik, M. Krompiec, R. Penczek, J. Mrzigod, A. Tórz, *J. Mol. Catal. A* **2006**, *253*, 132–146.
[14] L. D. Field, B. A. Messerle, K. Q. Vuong, P. Turner, *Dalton Trans.* **2009**, 3599–3614.
[15] a) *Circular Dichroism: Principles and Applications*, 2nd ed. (Eds.: N. Berova, K. Nakanishi, R. W. Woody), Wiley-VCH, Weinheim, Germany, **2000**; b) D. A. Lightner, J. E. Gurst, in: *Organic Conformational Analysis and Stereochemistry from Circular Dichroism Spectroscopy*, Wiley-VCH, Weinheim, Germany, **2000**; c) D. Casarini, L. Lunazzi, M. Mancinelli, A. Mazzanti, C. Rosini, *J. Org. Chem.* **2007**, *72*, 7667–7676; d) T. Mori, Y. Inoue, S. Grimme, *J. Phys. Chem. A* **2007**, *111*, 4222–4234; e) F. Ceccacci, G. Mancini, P. Mencarelli, C. Villani, *Tetrahedron: Asymmetry* **2003**, *14*, 3117–3122; f) N. Harada, A. Saito, N. Koumura, H. Uda, B. de Lange, W. F. Jager, H. Wynberg, B. L. Feringa, *J. Am. Chem. Soc.* **1997**, *119*, 7241–7248; g) C. Müller, E. A. Pidko, A. J. P. M. Staring, M. Lutz, A. L. Spek, R. A. van Santen, D. Vogt, *Chem. Eur. J.* **2008**, *14*, 4899–4905; h) J. J. M. Weemers, W. N. P. van der Graaff, E. A. Pidko, M. Lutz, C. Müller, *Chem. Eur. J.* **2013**, *19*, 8991–9004.
[16] R. S. Cahn, C. Ingold, V. Prelog, *Angew. Chem.* **1966**, *78*, 413–447; *Angew. Chem. Int. Ed. Engl.* **1966**, *5*, 385–415.
[17] G. D. Yadav, K. M. Devi, *Chem. Eng. Sci.* **2004**, *59*, 373–383.
[18] E. Santaniello, P. Ferraboschi, P. Grisenti, *Enzyme Microb. Technol.* **1993**, *15*, 367–382.
[19] N. Weber, E. Klein, K. D. Mukherjee, *Appl. Microbiol. Biotechnol.* **1999**, *51*, 401–404.
[20] G. D. Yadav, A. H. Trivedi, *Enzyme Microb. Technol.* **2003**, *32*, 783–789.
[21] R. J. Kaslauskas, A. N. E. Weissfloch, A. T. Rappaport, L. A. Cuccia, *J. Org. Chem.* **1991**, *56*, 2656–2665.
[22] A. M. M. Schreurs, X. Xian, L. M. J. Kroon-Batenburg, *J. Appl. Crystallogr.* **2010**, *43*, 70–82.
[23] Bruker SAINT-Plus, Bruker AXS Inc., Madison, Wisconsin (USA), **2001**.
[24] G. M. Sheldrick, *SADABS*, University of Göttingen, Germany, **1999**.
[25] G. M. Sheldrick, *Acta Crystallogr., Sect. A* **2008**, *64*, 112–122.
[26] A. L. Spek, *Acta Crystallogr., Sect. D* **2009**, *65*, 148–155.
[27] M. J. Frisch, G. W. Trucks, H. B. Schlegel, G. E. Scuseria, M. A. Robb, J. R. Cheeseman, G. Scalmani, V. Barone, B. Mennucci, G. A. Petersson, H. Nakatsuji, M. Caricato, X. Li, H. P. Hratchian, A. F. Izmaylov, J. Bloino, G. Zheng, J. L. Sonnenberg, M. Hada, M. Ehara, K. Toyota, R. Fukuda, J. Hasegawa, M. Ishida, T. Nakajima, Y. Honda, O. Kitao, H. Nakai, T. Vreven, J. A. Montgomery Jr, J. E. Peralta, F. Ogliaro, M. Bearpark, J. J. Heyd, E. Brothers, K. N. Kudin, V. N. Staroverov, R. Kobayashi, J. Normand, K. Raghavachari, A. Rendell, J. C. Burant, S. S. Iyengar, J. Tomasi, M. Cossi, N. Rega, J. M. Millam, M. Klene, J. E. Knox, J. B. Cross, V. Bakken, C. Adamo, J. Jaramillo, R. Gomperts, R. E. Stratmann, O. Yazyev, A. J. Austin, R. Cammi, C. Pomelli, J. W. Ochterski, R. L. Martin, K. Morokuma, V. G. Zakrzewski, G. A. Voth, P. Salvador, J. J. Dannenberg, S. Dapprich, A. D. Daniels, O. Farkas, J. B. Foresman, J. V. Ortiz, J. Cioslowski, D. J. Fox, *Gaussian 09*, revision A.01, Gaussian, Inc., Wallingford CT (USA), **2009**.
[28] T. Kanemitsu, A. Umehara, R. Haneji, K. Nagata, T. Itoh, *Tetrahedron* **2012**, *68*, 3893–3898.
[29] L. B. Schenkel, J. A. Ellman, *J. Org. Chem.* **2004**, *69*, 1800–1802.
[30] www.amtec-chemnitz.de.

Received: August 19, 2013
Published Online: November 19, 2013

